ORGANOMETALLICS

pubs.acs.org/Organometallics Article

Replacing Trimethylsilyl with Triisopropylsilyl Provides Crystalline (C₅H₄SiR₃)₃Th Complexes of Th(III) and Th(II)

Joseph Q. Nguyen, Lauren M. Anderson-Sanchez, William N. G. Moore, Joseph W. Ziller, Filipp Furche,* and William J. Evans*



Cite This: Organometallics 2023, 42, 2927-2937



ACCESS I

III Metrics & More

Article Recommendations

Supporting Information

ABSTRACT: The importance of the specific trialkylsilyl substituent in the cyclopentadienyl chemistry of $C_5H_4SiR_3$ ligands has been demonstrated by the synthesis of low oxidation-state thorium complexes. Although the structure of the disilyl-substituted cyclopentadienyl Th(III) complex, $[C_5H_3(SiMe_3)_2]_3Th^{III}(Cp''_3Th^{III})$, was reported in 1986, no monosilyl-substituted analogues, $(C_5H_4SiR_3)_3Th^{III}$ (R = alkyl, aryl), have been isolated to date, even though analogues are well known in U(III) chemistry. We now report that crystalline tris(monosilyl-substituted cyclopentadienyl) Th(III) and Th(II) complexes can be isolated when R = isopropyl, i.e., using the (triisopropylsilyl)cyclopentadienyl ligand, $C_5H_4Si^iPr_3$ (Cp^{TiPS}). The salt metathesis reaction between three equiv of KCp^{TiPS} and $Th^{IV}Br_4(DME)_2$ (DME = 1,2-



dimethoxyethane) afforded the colorless Th(IV) complex, $Cp^{TIPS}_{3}Th^{IV}Br$, 1, which was identified spectroscopically and crystallographically. KC_8 reduction of 1 in THF produced dark blue $Cp^{TIPS}_{3}Th^{III}$, 2, in crystalline form. The complex was identified by X-ray crystallography, EPR, and UV-visible spectroscopy in contrast to " $(C_3H_4SiMe_3)_3Th^{III}$ " which has never been isolated due to its instability. This Th(III) complex can be reduced further with KC_8 in the presence of 2.2.2-cryptand (crypt) to make $[K(crypt)][Cp^{TIPS}_3Th^{II}]$, 3, which is only the second crystallographically characterized Th(II) complex isolated since $(Cp''_3Th^{II})^{1-}$ was discovered in 2014. Spectroscopic, crystallographic, and density functional theory (DFT) analyses are consistent with $6d^1$ and $6d^2$ electron configurations for the Th(III) and Th(II) complexes, respectively. The importance of the triisopropylsilyl substituent and the role that steric factors play in the successful isolation of Th(III) and Th(II) complexes were evaluated by Guzei solid angle calculations and electrochemical studies. The results suggest that both electronic and steric effects should be considered in the isolation of Th(III) and Th(II) complexes.

INTRODUCTION

A crucial part of developing the chemistry and reactivity of any element in the periodic table is to have synthetic access to all of the available oxidation states. Generally, isolating coordination complexes containing metals in unusual oxidation states often depends on selecting stabilizing ligands that have suitable steric and electronic profiles. Optimizing the choice of ligands can be achieved by comparing similar metals and similar ligands.

Thorium and uranium chemistry has been advanced through this process since the two metals can display similar features. Despite this, thorium chemistry lags behind uranium chemistry in development, particularly in low oxidation-state chemistry. For example, scores of crystallographically characterized U(III) complexes have been known for several decades, $^{1-9}$ but it was not until 1986 that the first crystal structure of a Th(III) complex of any kind was reported by Lappert and co-workers, namely $[C_5H_3(SiMe_3)_2]_3Th^{III}$ (Cp″ $_3Th^{III}$). 10 Since then, only 10 other Th(III) complexes have been structurally characterized, Scheme 1. $^{11-20}$

The monosilyl-substituted cyclopentadienyl U(III) complex, $(C_5H_4SiMe_3)_3U^{III}$ (Cp'_3U^{III}), was also reported in 1986,³ but surprisingly, the monosilyl-substituted Th(III) analogue, Cp'_3Th^{III} , has never been isolated as it is not thermally stable enough to be crystallographically characterized.²¹

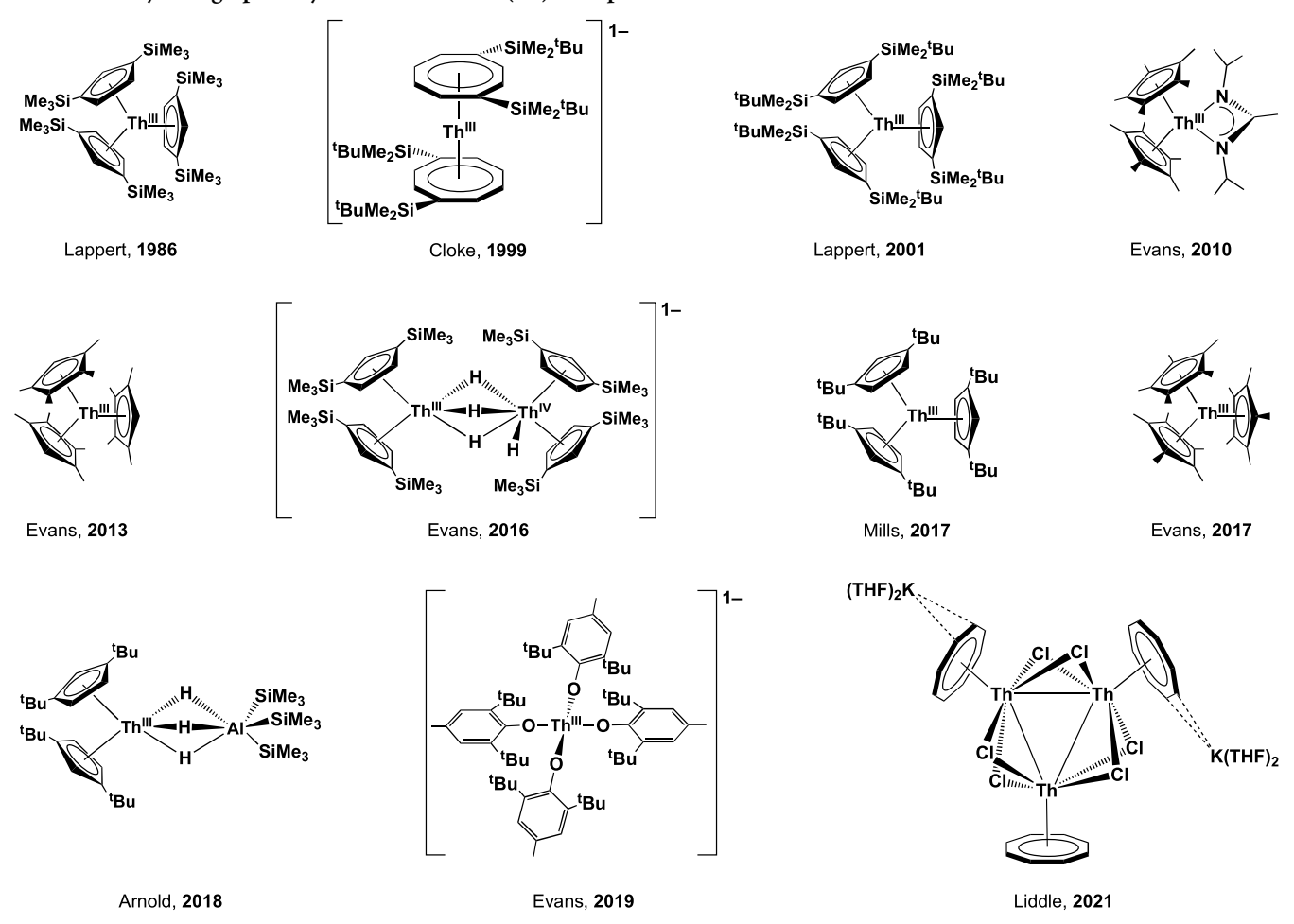
A similar situation exists in Th(II) and U(II) chemistry. The first example of a crystallographically characterized U(II) complex was reported in 2013, and numerous examples of other U(II) complexes with different ligand systems have been reported since then. $^{22-28}$ The first example of a molecular Th(II) complex, $(Cp''_3Th^{\rm II})^{1-}$, was isolated and crystallographically characterized in 2015, 29 but no other ligand

Received: August 1, 2023 Published: September 25, 2023





Scheme 1. Crystallographically Characterized Th(III) Complexes



environments have been found to stabilize a new Th(II) complex in the intervening eight years. This is particularly surprising since the $(Cp''_3Th^{II})^{1-}$ anion readily forms and has been isolated with five different alkali metal countercations, $[K(crypt)]^{1+}$, $[Rb(crypt)]^{1+}$, $[Cs(crypt)]^{1+}$, $[Na(18-crown-6)_2]^{1+}$, and $[K(18-crown-6)(THF)_7]^{1+}$.

Expanding the small library of low-valent Th(III) and Th(II) complexes is an important goal in understanding fundamental actinide chemistry. However, a major challenge in generating new examples of Th(II) complexes is the dearth of Th(III) precursor complexes. Furthermore, several of the fully characterized Th(III) complexes have polyalkylated cyclopentadienyl ancillary ligands which are less likely to yield stable Th(II) complexes compared to the relatively electron-withdrawing trialkylsilyl-substituted cyclopentadienyl ligands.³¹

Recent studies on Ln(II) aryloxide complexes (Ln = Y, La, Ce, Nd, Gd, Dy, Yb, and Lu) that highlighted the importance of steric bulk in stabilizing highly reducing Ln(II) ions ^{32,33} have provided precedent for us to explore the capacity of a larger mono(trialkylsilyl)-substituted cyclopentadienyl ligand, namely $(C_5H_4Si^iPr_3)^{1-}$, $(Cp^{TIPS})^{1-}$, to yield new isolable Th(III) and possibly Th(II) complexes. The synthetic, structural, spectroscopic, and electrochemical results from our study are reported here along with density functional theory (DFT) and Guzei solid angle calculations ³⁴ to evaluate steric trends.

RESULTS

The appropriate alkali metal cyclopentadienyl reagent, KC₅H₄Si¹Pr₃ (KCp^{TIPS}), was synthesized following a modified procedure from that developed by Cloke and co-workers for the synthesis of the disilyl-substituted analogue, NaC₅H₃(SiⁱPr₃)₂. 35 The monosilylcyclopentadienyl reagent was synthesized by slow addition of a solution of iPr₃SiOTf in hexane to a solution of NaC5H5 in THF at -78 °C followed by warming to room temperature and stirring for 3 h before work up, Scheme 2. The presence of bis(trialkylsilyl)cyclopentadiene byproducts is commonly observed during the synthesis of mono(trialkylsilyl)cyclopentadienes, so it is necessary to perform the addition slowly at low temperatures. 36,37 This was crucial for obtaining the crystalline thorium complexes described below. Extraction into hexane and filtration to remove the NaOTf byproduct yielded a pale-yellow oil that was presumed to be HCpTIPS in 86% yield. HCpTIPS can be treated with either KH in THF or KN(SiMe₃)₂ in toluene to generate KCp^{TIPS} in 75 and 83% yields, respectively (Scheme 2). The potassium salt was

Scheme 2. Synthesis of $KC_5H_4Si^iPr_3$ (KCp^{TIPS}) from NaC_5H_5

NaC₅H₅
$$\frac{{}^{+}{}^{i}Pr_{3}SiOTf}{THF/hexane, \\ -78 \degree C \text{ to RT}}{-NaOTf} \rightarrow HC_{5}H_{4}Si^{i}Pr_{3} \xrightarrow{toluene, RT} KC_{5}H_{4}Si^{i}Pr_{3}$$

$$\frac{{}^{+}KN(SiMe_{3})_{2}}{-HN(SiMe_{3})_{2}} \rightarrow KC_{5}H_{4}Si^{i}Pr_{3}$$

$$\frac{{}^{+}KN(SiMe_{3})_{2}}{-HN(SiMe_{3})_{2}} \rightarrow KC_{5}H_{4}Si^{i}Pr_{3}$$

$$\frac{{}^{+}KN(SiMe_{3})_{2}}{-HN(SiMe_{3})_{2}} \rightarrow KC_{5}H_{4}Si^{i}Pr_{3}$$

$$\frac{{}^{+}KN(SiMe_{3})_{2}}{-HN(SiMe_{3})_{2}} \rightarrow KC_{5}H_{4}Si^{i}Pr_{3}$$

identified by ¹H, ¹³C, and ²⁹Si NMR spectroscopy (Figures S1–S3).

The reaction between three equiv of KCp^{TIPS} and one equivalent of $Th^{IV}Br_4(DME)_2$ (DME = 1,2-dimethoxyethane) in diethyl ether at room temperature generated $Cp^{TIPS}_3Th^{IV}Br$, 1, eq 1, as a white solid in 85% yield. Complex 1 was characterized by analytical, spectroscopic, and crystallographic methods.

Initial attempts to crystallize 1 were unsuccessful until the methods described above were developed to improve the purity of the HCp TIPS starting material. Once this was done, crystallization was still challenging. Although colorless 1 is very soluble in hydrocarbon and arene solvents as well as diethyl ether, cooling the solutions to $-35\,^{\circ}$ C usually resulted only in the precipitation of powders. To obtain crystals of 1 suitable for study by X-ray diffraction, powders precipitated from a solution in toluene were separated and the more dilute mother liquor was stored at $-35\,^{\circ}$ C to induce further crystallization. After repeating this procedure several times, a relatively dilute solution of 1 in toluene (approximately 15 mg/4 mL) stored at $-35\,^{\circ}$ C overnight yielded crystals suitable for X-ray diffraction (Figure 1).

Complex 1 crystallizes in the $P\overline{1}$ space group, with a molecule of toluene in the asymmetric unit. The coordination environment about the thorium metal center is pseudotetrahedral with respect to the bromide ligand and the ring centroids of the three cyclopentadienyl ligands. The degree of distortion from tetrahedral can be evaluated by the sum of the three Cnt-Th-Cnt angles, which is 349° instead of the 360° expected for trigonal planar in tris(cyclopentadienyl)Th^{III} complexes and 328.5° expected for pure tetrahedral. The 2.55 Å average Cnt-Th distance of 1 falls within a range typically seen for other tris(cyclopentadienyl) Th(IV) complexes with halide ancillary ligands, such as $(C_5H_3^tBu_2)_3Th^{IV}Cl^{38}$ (2.600 Å), $Cp''_2(C_5Me_5)$ - $Th^{IV}Cl^{39}$ (2.571 Å), $Cp''_{3}Th^{IV}Cl^{39}$ (2.565 Å), $[C_{5}H_{3}(SiMe_{2}{}^{t}Bu)_{2}]_{3}Th^{IV}Cl^{39}$ (2.581 Å), $(C_{5}Me_{4}H)_{3}Th^{IV}Br^{17}$ (2.576 Å), and $(C_5H_4SiMe_3)_3Th^{IV}Br^{40}$ (2.535 Å). Also, the Th-Br distance of 2.8310(9) Å is comparable with the Th-Br distances of the structurally similar (C₅Me₄H)₃Th^{IV}Br¹⁷ (2.8372(8) Å) and $(C_5H_4SiMe_3)_3Th^{IV}Br^{40}$ (2.8355(8) Å).

Treating complex 1 with 1.2 equiv of KC_8 in THF at room temperature immediately generated a dark blue solution, similar to that of $Cp''_3Th^{III\,10}$, and a black precipitate, presumably graphite. Upon removal of solvent under reduced pressure, the reduction product was extracted into hexane, dried, and triturated with $SiMe_4$ to yield $Cp^{TIPS}_3Th^{III}$ as a royal blue solid in 98% yield, eq 2. The reaction can also be performed in diethyl ether, but the reaction proceeds at a slower rate.

The EPR spectrum of a solution of **2** in THF at 77 K displays an axial signal with g_{\parallel} = 1.97 and g_{\perp} = 1.88. At room temperature, that same solution displays an isotropic EPR signal with $g_{\rm iso}$ = 1.90 (Figure 2). These values are consistent with other reported crystallographically characterized Th(III) complexes, as shown in Table 1. Due to the paramagnetism of the Th(III) ion, the ¹H

$$ThBr_{4}(DME)_{2} \xrightarrow{+3 \text{ KCp}^{TIPS}} -3 \text{ KBr}$$

$$i_{Pr_{3}Si} \xrightarrow{i_{Pr_{3}Si}} Th_{Si}^{IV} p_{r_{3}}$$

$$(1)$$

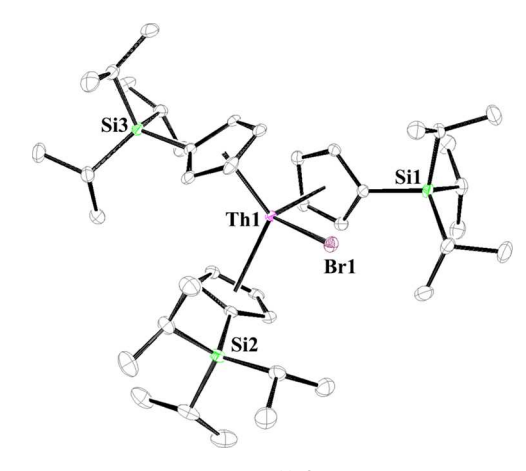


Figure 1. Molecular structure of $Cp^{\mathrm{TIPS}}_3\mathrm{Th^{IV}Br}$, 1, with selective atom labeling. Ellipsoids are drawn at the 50% probability level, and the cocrystallized toluene molecule and hydrogen atoms are not shown for clarity.

$$\begin{array}{c|c} Si^{i}Pr_{3} & Si^{i}Pr_{3} \\ \hline Th^{I_{3}} & \hline \\ Br & Si^{i}Pr_{3} \\ \hline \\ Br & Si^{i}Pr_{3} \\ \hline \end{array}$$

NMR and 13 C NMR spectra of **2** could not be definitively assigned (Figures S9 and S10). However, the 29 Si NMR spectrum of **2** shows a resonance at -21.8 ppm (Figure S11).

The UV-visible spectrum of **2** contains absorptions at 504, 582, and 664 nm with extinction coefficients of 1300, 900, and 1100 M⁻¹cm⁻¹, respectively, and a shoulder at 350 nm with an extinction coefficient of 844 M⁻¹cm⁻¹ (Figure 3). As shown, this spectrum is similar to that of the crystallographically characterized Th(III) complex, Cp″₃Th. ¹² In addition, the infrared spectrum of **2** is almost identical to that of complex **1** since M-Br vibrations appear below 650 cm⁻¹ (Figures S23 and S24). ⁴²

Storage of a saturated solution of **2** in pentane overnight at $-35\,^{\circ}\mathrm{C}$ generated large dark blue blocks of $\mathrm{Cp^{TIPS}}_{3}\mathrm{Th^{III}}$ suitable for study by X-ray diffraction, Figure 4, in stark contrast to " $\mathrm{Cp'}_{3}\mathrm{Th^{III}}$ " which has never been isolated. Complex **2** crystallizes in the $P\overline{1}$ space group, with a single molecule in the asymmetric unit. Unlike **1**, the structure of **2** has a trigonal planar arrangement of the three $\mathrm{Cp^{TIPS}}$ rings around the thorium metal center with a sum of the $\mathrm{Cnt-Th-Cnt}$ (Cnt = ring centroid) angles of 359.4° that matches the 360° sum of angles found for the other tris(cyclopentadienyl) Th(III) complexes. 10,12,14,17,19 The average Cnt—Th distance of 2.520 Å is equivalent to that of $\mathrm{Cp''}_{3}\mathrm{Th^{III10}}$ (2.518 Å) and numerically shorter than that of $[\mathrm{C_{5}H_{3}}(\mathrm{Si'BuMe_{2}})_{2}]_{3}\mathrm{Th^{III12}}$ (2.533 Å), ($\mathrm{C_{5}Me_{4}H})_{3}\mathrm{Th^{III17}}$ (2.551 Å), ($\mathrm{C_{5}H_{3}'Bu_{2}})_{3}\mathrm{Th^{III19}}$ (2.566 Å), and ($\mathrm{C_{5}Me_{5}})_{3}\mathrm{Th^{III14}}$ (2.62 Å). A full table of metrical parameters for **2** can be found in the Supporting Information.

When a solution of **2** and 2.2.2-cryptand (crypt) in THF was treated with 1.2 equiv of KC₈, an inky dark blue-black color was generated. After filtration to remove insoluble solids, dark blue-black solids were obtained from the filtrate upon removal of the solvent *in vacuo*. Unlike complex **2**, these solids are insoluble in hydrocarbon solvents and were washed with hexane to remove unreacted complex **2**. Although some attempts to isolate the

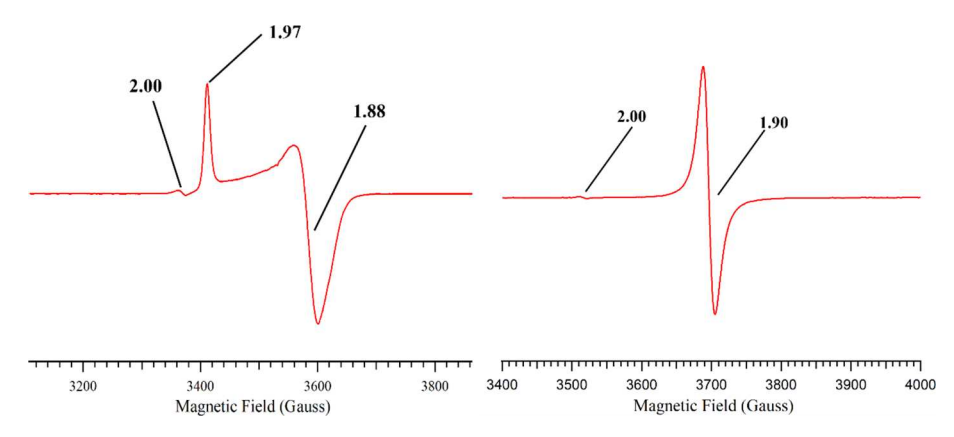


Figure 2. X-band EPR of $Cp^{TIPS}_{3}Th^{III}$ in THF at 77 K (left; mode: perpendicular) and at room temperature (right; mode: perpendicular). The feature observed at g = 2.00 for both spectra is attributed to electride. 41

Table 1. EPR Data for Th(III) Complexes along with Calculated Guzei G Values (G) (Discussed Later) Presented in Increasing Order

Th(III)/Th(II) complex	$g_{ m iso}$	$g_{ }$	g_{\perp}	G(%)
$(C_5Me_5)_3Th^{III14}$	1.88	1.97	1.85	79
$(C_5Me_4H)_3Th^{III17}$	1.92			82
$(C_5Me_5)_2Th^{III}(^iPrNC(Me)N^iPr)^{16}$	1.871	1.97	1.91	84
$[K(THF)_5(Et_2O)][Th^{III}(OC_6H_2-2,6^{-t}Bu_2-4-Me)_4]^{11}$	1.84	1.99	1.79	87
$(C_5H_4SiMe_3)_3Th^{III*21}$	1.90	1.98	1.89	87 ^a
$(C_5H_3{}^tBu_2)_3Th^{III19}$		1.974	1.880	88
$[K(DME)_2][C_8H_6(Si^tBuMe_2)_2]_2Th^{III15}$	1.916			88
$[K(crypt)][Cp^{TIPS}_{3}Th^{II}]^{b}$				87 ^c , 88 ^d
$Cp^{TIPS}_{3}Th^{IIIb}$	1.90	1.97	1.88	89
$[K(crypt)][Cp''_2Th^{III}(\mu-H)_3Th^{IV}HCp''_2]^{13}$				89
$[K(crypt)][Cp''_3Th^{II}]^{29}$				90
$Cp''_{3}Th^{III12}$	1.910	1.97	1.88	91
$[K(crypt)][Cp''_{2}Th^{III}(\mu-H)_{3}Th^{IV}HCp''_{2}]^{13}$				91

"Calculated from a DFT-calculated structure. bThis work. $^c[K(crypt)][Cp^{TIPS}_3Th]$ grown from Et₂O. $^d[K(crypt)][Cp^{TIPS}_3Th]$ grown from THF/hexane.

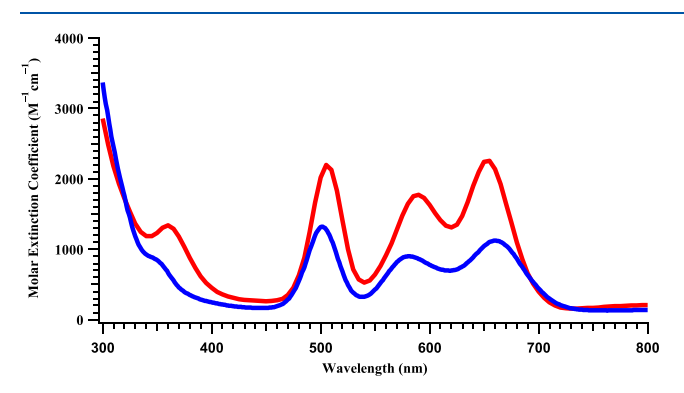


Figure 3. UV–visible spectra of 2 (blue) and ${\rm Cp''}_3{\rm Th^{III}}$ (red) in THF at room temperature.

reduction product by crystallization from diethyl ether or THF/hexane led to the isolation of colorless crystals of the ligand salt, $[K(crypt)][Cp^{TIPS}]$, identified by X-ray crystallography (see Supporting Information), crystallization from either a diethyl

$$Th^{\coprod} \xrightarrow{Si'Pr_3} \xrightarrow{THF} + KC_8 + 2.2.2-cryptand - graphite} \xrightarrow{Pr_3Si} \xrightarrow{Si'Pr_3} \begin{bmatrix} Si'Pr_3 \\ - Si'Pr_3 \end{bmatrix}$$

$$[Pr_3Si] \xrightarrow{Si'Pr_3} \xrightarrow{Si'Pr_3} \begin{bmatrix} Si'Pr_3 \\ - Si'Pr_3 \end{bmatrix}$$

$$[Pr_3Si] \xrightarrow{Si'Pr_3} \xrightarrow{Si'Pr_3} \begin{bmatrix} Si'Pr_3 \\ - Si'Pr_3 \end{bmatrix}$$

$$[Pr_3Si] \xrightarrow{Si'Pr_3} \xrightarrow{Si'Pr_3} \begin{bmatrix} Si'Pr_3 \\ - Si'Pr_3 \end{bmatrix}$$

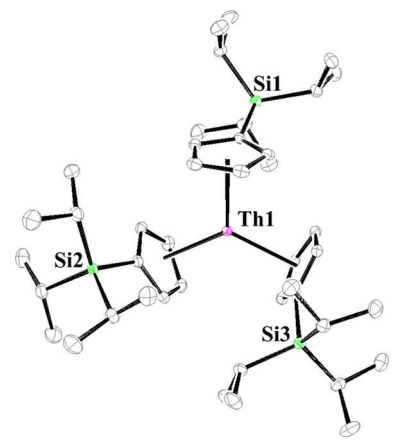


Figure 4. Molecular structure of $Cp^{TIPS}_3Th^{III}$ with selective atom labeling. Ellipsoids are drawn at the 50% probability level and hydrogen atoms are not shown for clarity.

ether solution over 2 weeks or from a THF/hexane solution over 2 days at -35 °C yielded dark blue-black crystals of $[K(crypt)][Cp^{TIPS}_{3}Th^{II}]$, 3, identified by X-ray crystallography (Figure 5 and eq 3).

Complex 3 crystallizes in two different unit cells depending on the crystallization conditions. From a saturated solution of THF/hexane stored at -35 °C, 3 crystallizes in the $P2_1/c$ space

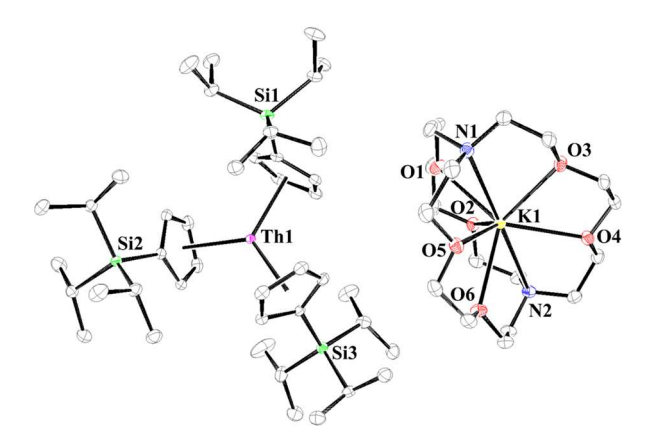


Figure 5. Molecular structure of $[K(crypt)][Cp^{TIPS}_3Th^{II}]$, 3, with selective atom labeling. Ellipsoids are drawn at the 50% probability level and hydrogen atoms are not shown for clarity.

group. The structure of 3 consists of a $[K(crypt)]^{1+}$ cation that is well separated from a $(Cp^{TIPS}{}_3Th^{II})^{1-}$ anion. The $(Cp^{TIPS}{}_3Th^{II})^{1-}$ anion in 3 has a trigonal planar arrangement of the three Cp^{TIPS} rings around the thorium atom with a sum of 359.5° for the Cnt–Th–Cnt angles, similar to the 360° values reported for the previously characterized structures of the $(Cp''{}_3Th^{II})^{1-}$ anion. 29 The average Th–Cnt distance of 2.521 Å in complex 3 is equivalent to that of $Cp^{TIPS}{}_3Th^{III}$, just as the average Th–Cnt distances of 2.521 Å in $[K(crypt)]-[Cp''{}_3Th^{III}]^{29}$ and 2.525 Å in $[K(18\text{-crown-6})(THF)_2]-[Cp''{}_3Th^{III}]^{29}$ are equivalent to the average Th–Cnt distance in their Th(III) precursor, $Cp''{}_3Th^{III}$. In these Th(III)/Th(II) pairs, the bond distance to the ligand does not change significantly upon reduction. $^{29,43-46}$

When X-ray quality crystals are grown from a saturated diethyl ether solution stored at $-35\,^{\circ}$ C, complex 3 crystallizes in the $P2_1/n$ space group. The structural parameters of the $P2_1/n$ structure of 3 are similar to those of the $P2_1/c$ structure with an average Th–Cnt distance of 2.516 Å and a sum of 359.9° for the Cnt–Th–Cnt angles. However, the relative orientations of the rings and silyl substituents are not equivalent between the two structures of 3 and do not superimpose (Figure 6). This shows the flexibility of the Cp^{TIPS} ligands to form X-ray quality crystals in more than one orientation. Full tables of bond distances and angles for both structures of complex 3 is given in the Supporting Information.

The reduction of Cp^{TIPS}₃Th^{III}, **2**, with KC₈ without the presence of a chelate also generated blue-black solutions similar to those of **3**, but once the solvent was removed, the resulting blue-black solids were poorly soluble in THF. Once dissolved, the solutions quickly become colorless. This result highlights the importance of the alkali metal chelate in the successful isolation of **3**.

The EPR spectrum of complex 3 is silent at 77 K, similar to that of the originally reported EPR spectrum for $(Cp''_3Th^{II})^{1-}$ (Figure S27). Pindeed, H, C, and SS NMR spectra can be collected for complex 3 in THF- d_8 , and resonances were observed in the diamagnetic region, shifted slightly in comparison to the NMR spectra of KCp^{TIPS} and [K(crypt)]-[Cp^{TIPS}] (see Supporting Information). In comparison to the resonance observed at -6 ppm in the SS NMR of [K(crypt)]-[Cp''_3Th^{II}], complex 3 shows a resonance at -5.5 ppm versus SiMe₄.

Complex 3 decomposes faster at room temperature than the previously reported Th(II) complex, $[K(18-crown-6)(THF)_2]$ -

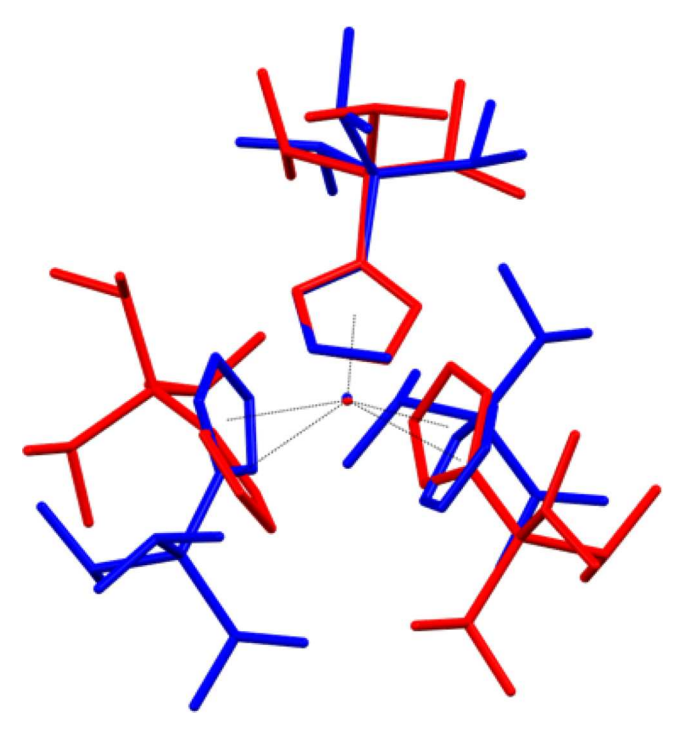


Figure 6. Overlay of the $P2_1/n$ (blue) and $P2_1/c$ (red) structures of the anion of $[K(\text{crypt})][Cp^{\text{TIPS}}_3\text{Th}^{\text{II}}]$, 3. Hydrogen atoms are not shown for clarity. Both structures are oriented to have an exact overlay of the thorium metal center and one cyclopentadienyl ring. The two structures are not optical isomers although the orientations of the ligands differ along those lines (see Figure S26).

[Cp" $_3$ Th^{II}], which decomposes only 8% after 8 days at 298 K in THF. 29 In contrast, THF- 4 8 solutions of complex 3 stored under an argon atmosphere in J. Young NMR tubes at ambient temperature completely lose their color to clear pale-yellow solutions after 4 days (Figures S28–S31). At that point, the 1 H, 13 C, and 29 Si NMR spectra of the resulting solution showed the presence of a new diamagnetic species which may be a Th(IV) hydride complex based on the resonance observed at 11.83 ppm in the 1 H NMR (Figures S15 and S16). Similar Th(IV) hydride products were observed in attempts to reduce (C_5 Me $_4$ H) $_3$ Th^{III} with KC $_8$ in the presence of crypt which led to the identification of (C_5 Me $_4$ H) $_3$ Th^{IV}H, [K(crypt)]-{(C_5 Me $_4$ H) $_2$ Th^{IV}H[η^5 : η^1 -C $_5$ Me $_3$ H(CH $_2$)]}, and [K(crypt)]-[C_5 Me $_4$ H] as the only isolable products. Similar 13

The UV-visible spectrum of complex 3 is compared to that of 2 in Figure 7. The measured extinction coefficients of 3900, 4700, and 5200 M⁻¹ cm⁻¹ for the absorptions centered at 424, 585, and 650 nm are likely to be underestimated due to decomposition, but they clearly are more intense than those of complex 2 (Figure 7). However, the measured extinction coefficients of 3 are not as large as the 23,000 M⁻¹ cm⁻¹ value observed for the absorption at 650 nm of [K(crypt)]-[Cp"₃Th^{II}].²⁹

Attempts to measure the electrochemical behavior of the blue $Cp^{TIPS}{}_3Th^{III}$ in our hands were complicated by the fact that it decomposes to a colorless solution upon addition to electrolyte solutions of $[^nBu_4N][BPh_4]$ or $[^nBu_4N][PF_6]$ in THF. Although 2 decomposed in the supporting electrolyte solution, the voltammogram of $Cp^{TIPS}{}_3Th^{IV}Br$, 1, could be obtained using approximately 100 mM multiply recrystallized $[^nBu_4N][BPh_4]$ supporting electrolyte concentrations in THF. Scanning anodically, a redox process centered at -3.09 V vs Fc^+/Fc was

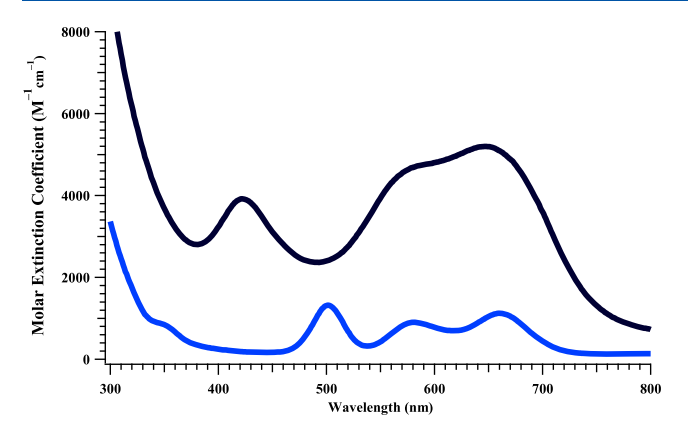


Figure 7. UV—visible spectra of **2** (blue trace) and **3** (blue-black trace) in THF at room temperature.

observed, which was assigned as the Th(IV)/Th(III) couple (Figure 8). The voltammogram of 1 was complicated by redox processes presumed to be ligand-based events, Figure S32, so 20 cycles were performed between -1.92 and -3.82 V to more accurately determine the Th(IV)/Th(III) redox couple of 1.

The Th(IV)/Th(III) reduction potential of 1 is more negative than that of the $Cp''_3Th^{IV}X$ (X = Cl, Br) complexes, which contain disilyl-substituted cyclopentadienyl ligands but similar to the redox couple of the Th^{IV} complex, Cp'₃Th^{IV}Cl, which contains monosilyl-substituted cyclopentadienyl ligands (Table 2). Furthermore, compared to the Th(IV)/Th(III) reduction potential of (C₅Me₄H)₃Th^{IV}Br, which contains polyalkylated cyclopentadienyl ligands, complex 1 and all of the other tris(silylcyclopentadienyl) Th^{IV} complexes have noticeably more positive Th(IV)/Th(III) redox couples. This trend is in line with the electron-withdrawing nature of silyl groups relative to alkyl groups in complexes of this type.³¹ The Th(IV)/Th(III) reduction potential does not change significantly upon substitution of the SiMe₃ substituent with the more sterically encumbering SiⁱPr₃ substituent. This suggests that the number of the trialkylsilyl substituents on the cyclopentadienyl ligands has a more significant effect on the Th(IV)/Th(III) redox couple than the specific trialkylsilyl group. Hence, the increased thermal stability of $Cp^{TIPS}_{3}Th^{III}$ compared to the reduction product of $Cp'_{3}Th^{IV}X^{21}$ is possibly due to steric saturation about the metal center and not a difference in reduction potentials.

Electronic structure calculations on both $Cp^{TIPS}_3Th^{III}$ and $(Cp^{TIPS}_3Th^{II})^{1-}$ were performed using DFT with the TPSSh

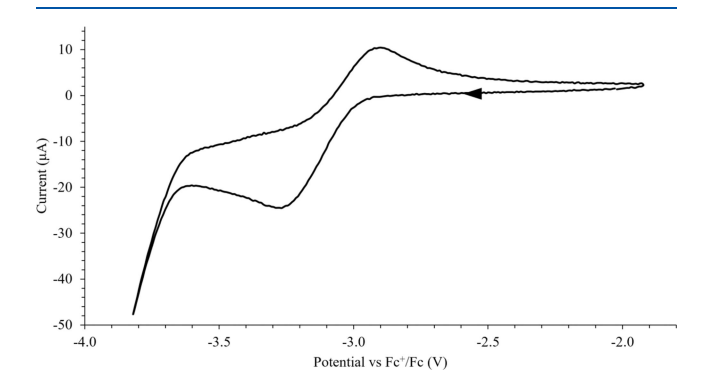


Figure 8. Voltammogram of $Cp^{TIPS}_3Th^{IV}Br$, **1**, at $\nu=200$ mV s⁻¹ in 100 mM ["Bu₄N][BPh₄]/THF at room temperature after 20 cycles scanned between -1.92 and -3.82 V.

Table 2. Reduction Potentials of Tris(cyclopentadienyl)thorium Complexes with 100 mM ["Bu₄N][BPh₄] Supporting Electrolyte in THF in Increasing Order of $E_{1/2}$

Th(IV) complex	$E_{PC}(V)$	$E_{\mathrm{PA}}\left(\mathrm{V}\right)$	$E_{1/2}$ (V)
Cp" ₃ Th ^{IV} Br ³⁰	-3.00	-2.77	-2.89
Cp" ₃ Th ^{IV} Cl ³⁰	-3.04	-2.81	-2.93
$Cp^{TIPS}_{3}Th^{IV}Br^{a}$	-3.27	-2.90	-3.09
Cp′ ₃ Th ^{IV} Cl ³⁰	-3.38	-2.90	-3.14
Cp′ ₃ Th ^{IV} Br ³⁰	-3.17		
$(C_5Me_4H)_3Th^{IV}Br^{30}$	-3.48	-3.19	-3.34
^a This work.			

hybrid meta-generalized gradient density functional⁴⁷ with the D3 dispersion correction ^{48,49} and the resolution of the identity (RI-J) approximation.⁵⁰ Scalar relativistic effective core potentials with the def-TZVP basis set ⁵¹ were used for thorium, and the polarized split-valence basis set def2-SV(P) was used for other atoms.⁵² The continuum solvent model COSMO⁵³ was used with parameters for THF (dielectric constant ε = 7.52 and refractive index $R_{\rm ind}$ = 1.41).⁵⁴ All calculations were performed with the TURBOMOLE package V7.6.^{55,56} Complete details can be found in the Supporting Information.

The geometry-optimized structures of the neutral $Cp^{TIPS}_{3}Th^{III}$ and the $(Cp^{TIPS}_{3}Th^{III})^{1-}$ anion have average Th—Cnt distances of 2.501 and 2.489 Å, respectively, which are within 0.03 Å of the experimentally determined Th—Cnt average distances, 2.520 and 2.524 Å, respectively. The calculated bond angles are also reproduced within a few degrees for both structures. Geometry optimization on the coordinates for both structures yields ground state geometries with C_1 -symmetry.

The electronic structure suggests $(6d_{22})^1$ and $(6d_{22})^2$ electron configurations for $Cp^{TIPS}_3Th^{III}$ and $(Cp^{TIPS}_3Th^{II})^{1-}$, respectively. These are the same ground-state electron configurations assigned to the neutral Cp''_3Th^{III} and the anionic $(Cp''_3Th^{II})^{1-}$ of the disilyl-substituted cyclopentadienyl analogues. To further verify the ground-state configuration of $(Cp^{TIPS}_3Th^{II})^{1-}$, geometry optimization was run on the same anion constrained to a triplet state. The total energy was >0.4 eV higher than the singlet ground state. The $6d_{22}$ character of the HOMO for $(Cp^{TIPS}_3Th^{II})^{1-}$ can be seen in Figure 9.

Time-dependent DFT calculations were then conducted on the geometry-optimized structures, and the resulting simulated UV—visible absorption spectra qualitatively reproduce the experimental spectra observed (Figure 10). For $Cp^{\rm TIPS}_{\ 3}Th^{\rm III}$, the strongest absorptions >550 nm primarily correspond to 6d \rightarrow 5f transitions. For $(Cp^{\rm TIPS}_{\ 3}Th^{\rm II})^{1-}$, the three absorptions between 450 and 650 nm with the greatest oscillator strengths correspond to d \rightarrow f and/or d \rightarrow p transitions. While further improvement of the agreement between experimental and computational spectra for 2 might be possible, the observed deviations are within the expected range for this type of calculation and measurement.

The importance of steric saturation of the metal center in Th(III) and Th(II) complexes was evaluated using the Guzei solid angle method that provides G, an estimation of the percentage of the coordination sphere of the metal that is protected by the ligands.³⁴ Guzei G values were calculated for complexes 2 and 3 in addition to all of the crystallographically characterized Th(III) and Th(II) complexes, which have published crystal structures that include hydrogen atoms (Table 1). Although it is generally best to compare G values

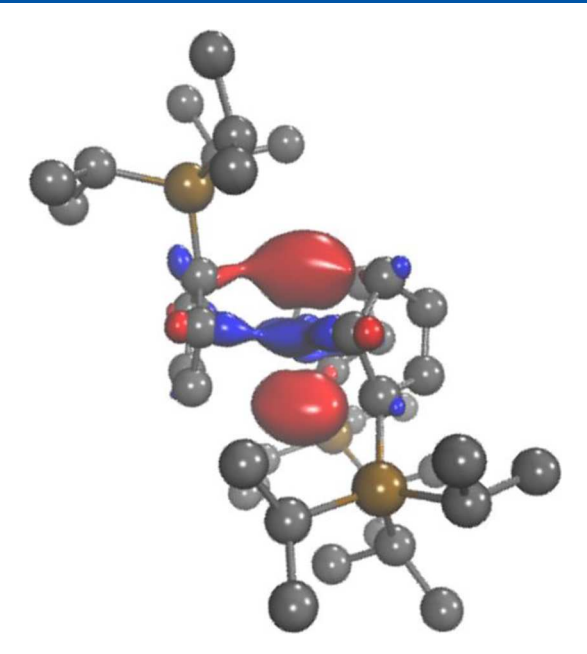
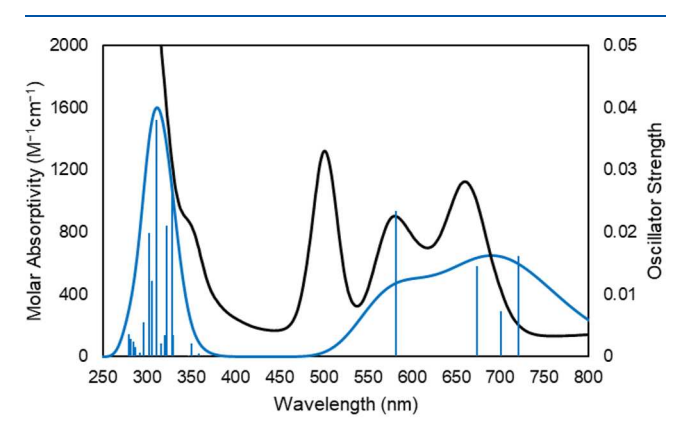


Figure 9. Calculated HOMO (ε = -1.235) of $(Cp^{TIPS}_3Th^{II})^{1-}$ plotted with a contour value of 0.05.



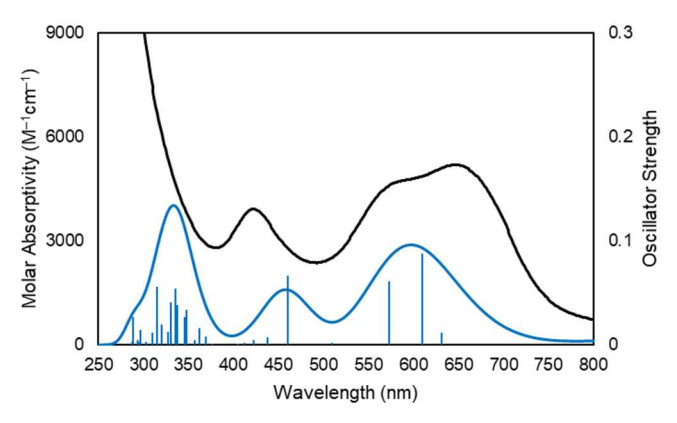


Figure 10. Simulated (blue) and experimental (black) UV–visible spectra for $Cp^{TIPS}_{3}Th^{III}$, **2** (top), and $[K(crypt)][Cp^{TIPS}_{3}Th^{II}]$, **3** (bottom). The computed TDDFT oscillator strengths are shown as blue vertical lines. Each calculated spectrum was empirically blue-shifted by 0.30 eV, and a Gaussian line broadening of 0.15 eV was applied.

only for a structurally similar series of complexes, all of the isolable Th(III) complexes regardless of ligand have G values between 82 and 91%, except $(C_5Me_5)_3Th^{III}$. This defines a

range of G values that can provide stable structures. The low value of 79% observed for $(C_5Me_5)_3Th^{III}$ can be rationalized by the fact that the Th–Cnt distances reported for this complex are substantially longer than those observed for other complexes as is characteristic of $(C_5Me_5)_3M^{III}$ complexes. This causes the $(C_5Me_5)^{1-}$ ligands to be located further from the metal center, which leads to a lower G value.

The new Th(III) complex, **2**, has a G value of 89%, whereas the new Th(II) complex, **3**, has G values of 87 and 88%, falling within the range of those calculated for the other Th(III) and Th(II) complexes in the literature. The small decrease in the G value upon reduction from Th(III) in **2** to Th(II) in **3** is consistent with small changes in metal—ligand distances upon the addition of a 6d electron. Similarly, the G values for Cp''_3Th^{III} and $(Cp''_3Th^{II})^{1-}$ are 91 and 90%, respectively.

Although complexes 2 and 3 have *G* values in the range typical of stable complexes, G values alone cannot always predict stability even within a class of structurally similar complexes. This is exemplified by theoretical calculations conducted on the monotrimethylsilyl-substituted cyclopentadienyl Th(III) complex, (Cp'3Th^{III}. A G value of 87% was calculated for this complex using a DFT-calculated structure, which suggests that it should be isolable. However, no experimental evidence of its formation has been observed to date. 21 We note here that a G value for Cp^{TIPS}₃Th^{III} was calculated to be 93% from a DFT -calculated structure prior to the crystallization of 2, which provided an experimental value of 88%. Hence, G calculations based on DFT structures may be slightly overestimated, and the actual value for Cp'₃Th^{III} could be at the lower limit of the range cited above. In addition, slight differences in the way molecules pack in the solid state can also introduce variations in the G value. This is exemplified by the 87 and 88% G values for the two crystal structures of [K(crypt)][CpTIPS3ThII], 3, grown under different conditions, as shown in Figure 6.

Since the other tris(ligand) Th(III) complexes with polyalkylated cyclopentadienyl ligands, (C5Me5)3ThIII, $(C_5Me_4H)_3Th^{III}$, and $(C_5Me_5)_2Th^{III}$ [PrNC(Me)N'Pr], have G values of 79, 82, and 84%, respectively, it is conceivable that reductions of these Th(III) complexes would form isolable Th(II) complexes. Although reductions of these Th(III) complexes form transient dark green solutions similar to that of $(\tilde{Cp''}_3Th^{II})^{1-}$, none of these reactions yielded isolable Th(II) products. 58 In the case of (C₅Me₄H)₃Th^{III}, only the Th(IV) C-H bond activation product, [K(crypt)]{[C₅Me₄H]₂Th^{IV}H- $[\eta^5:\eta^1-C_5Me_3H(CH_2)]$, and the Th(IV) hydride complex, (C₅Me₄H)₃Th^{IV}H, were isolated and characterized.¹³ In these cases, it is possible that the electron-donating ability of the ligands is making them more reactive, and this should be considered in addition to the steric bulk of the cyclopentadienyl ligand when seeking isolable Th(II) complexes.

CONCLUSIONS

In summary, replacing trimethylsilyl with triisopropylsilyl as the trialkylsilyl substituent on the cyclopentadienyl ligand has led to the isolation of the first crystalline monosilyl-cyclopentadienyl Th(III) complex and the second example of a Th(II) complex of any kind. Specifically, $Cp^{TIPS}_{3}Th^{III}$, **2**, and [K(crypt)]-[$Cp^{TIPS}_{3}Th^{III}$], **3**, can be isolated and structurally characterized, while the isolation of $Cp'_{3}Th^{III}$ and $[Cp'_{3}Th^{III}]^{1-}$ has been elusive. The synthetic utility of the $Si'Pr_{3}$ functional group compared to $SiMe_{3}$ has been long ago documented in organic chemistry. However, this is surprising in this case since the alkyl groups on the silyl substituents are not close to the metal

center and the 89% G value for $\operatorname{Cp^{TIPS}}_3\operatorname{Th^{III}}$ is close to the 87% value estimated for $\operatorname{Cp'}_3\operatorname{Th^{III}}$. The superiority of the triisopropylsilylcyclopentadienyl ligand for isolating $\operatorname{Th}(\operatorname{III})$ and $\operatorname{Th}(\operatorname{II})$ complexes emphasizes the importance of ligand variation in optimizing chemistry. In addition, the successful isolation of complex 3 exemplifies the fact that $\operatorname{Th}(\operatorname{II})$ complexes are not limited to bis(trialkylsilyl)cyclopentadienyl coordination environments if the monotrialkylsilyl substituent is large enough. Clearly, the interplay of electronic and steric factors that stabilize $\operatorname{Th}(\operatorname{III})$ and $\operatorname{Th}(\operatorname{II})$ complexes remains to be fully defined.

EXPERIMENTAL DETAILS

Caution! ²³²Th is an α emitter with a half-life of approximately 1.41 \times 10¹⁰ years. Samples should be prepared and handled only in laboratories appropriately equipped to handle radioactive materials.

All manipulations and syntheses described below were conducted with the rigorous exclusion of air and water using standard Schlenk line and glovebox techniques under an argon atmosphere. Solvents were sparged with UHP argon, dried by passage through columns containing Q-5 and molecular sieves, and stored over activated sieves overnight prior to use. Deuterated NMR solvents were degassed and dried over activated 3 Å molecular sieves overnight prior to use. ¹H NMR, ¹³C NMR, and ²⁹Si NMR spectra were recorded on a Bruker AVANCE600 MHz spectrometer at 298 K unless otherwise stated. ¹H NMR and ¹³C NMR spectra were referenced internally to residual protiosolvent resonances, and ²⁹Si NMR spectra were referenced internally to SiMe₄. Infrared spectra were recorded as compressed solids on an Agilent Cary 630 ATR-FTIR spectrometer. UV-visible spectra were collected under an inert atmosphere of argon in THF at 298 K using a Varian Cary 50 Scan UV-visible spectrometer in a 1 mm Schlenk cuvette fitted with a Teflon stopper unless otherwise stated. X-band EPR spectra were recorded on a Bruker EMX spectrometer equipped with an ER041Xg microwave bridge and calibrated with DPPH (g = 2.0036). Elemental analyses were conducted on a Thermo Scientific FlashSmart CHNS/O elemental analyzer at UC Irvine Materials Research Institute's TEMPR facility in Irvine, California. $NaC_5H_5^{60}$ and KC_8^{61} were synthesized according to the literature procedures. $Th^{IV}Br_4(DME)_2$ (DME = 1,2dimethoxyethane) was synthesized by treating Th^{IV}Br₄(THF)₄⁶² with neat DME followed by filtration and drying under reduced pressure. Triisopropylsilyl triflate was purchased from TCI Chemicals and used as received. 2.2.2-Cryptand (crypt) was purchased from Sigma-Aldrich and recrystallized in Et₂O prior to use.

Synthesis of $KC_5\bar{H}_4S\bar{i}'Pr_3$ from NaC_5H_5 . In separate Schlenk flasks, solutions of NaC_5H_5 (2.01 g, 22.8 mmol) in THF (50 mL) and iPr_3SiOTf (7.06 g, 306.42 mmol) in hexane (20 mL) were cooled to -78 °C. The iPr_3SiOTf solution was then added dropwise over 2 h to the NaC_5H_5 solution via cannula, and the resulting mixture was allowed to stir and warm to room temperature over 3 hours, at which point it became a pale-yellow mixture with much colorless precipitate. Solvent was removed under reduced pressure to yield a pale-yellow residue. The flask was then brought into a glovebox, and the residue was extracted into hexane (20 mL), centrifuged, and filtered to remove insoluble solids, presumably NaOTf. Solvent was removed under reduced pressure to yield a yellow oil, presumably $HC_5H_4Si^iPr_3$ (4.37 g, 86%), which was directly used for the next step.

HC₅H₄Si¹Pr₃ (1.22 g, 5.46 mmol) was dissolved in toluene (3 mL) to afford a pale-yellow solution. With stirring, a solution of KN(SiMe₃)₂ (1.04 g, 23.05 mmol) in toluene (15 mL) was added dropwise at room temperature over 10 min. Colorless precipitate slowly formed throughout the addition, and the mixture was allowed to stir at room temperature overnight. The mixture was filtered through a medium porosity glass frit, and the solids were washed with toluene (5 mL) followed by hexane (20 mL). The solids were collected and dried in vacuo to yield KC₅H₄Si¹Pr₃ as white powdery solids (1.03 g, 76%). ¹H NMR (THF- d_8 , 600 MHz): δ 5.96–5.95 (m, 2H, C₅H₄Si¹Pr₃), 5.83–5.82 (m, 2H, C₅H₄Si¹Pr₃), 1.18–1.13 (sept, 3 J_{HH} = 1.1 Hz, 3H, CH of ¹Pr), 1.07–1.06 (d, 3 J_{HH} = 1.1 Hz, 18H, CH₃ of ¹Pr). ¹³C NMR (THF- 3 C NMR (THF- 3 C) NMR (THF- 3

 $d_{8},~151~\text{MHz}):~\delta~115.1~~(C_{5}H_{4}\text{Si}^{\prime}\text{Pr}_{3}),~108.0~~(C_{5}H_{4}\text{Si}^{\prime}\text{Pr}_{3}),~103.1~~(C_{5}H_{4}\text{Si}^{\prime}\text{Pr}_{3}),~20.1~~(CH_{3}~\text{of}^{\prime}\text{Pr}),~13.4~~(CH~\text{of}^{\prime}\text{Pr}).~^{29}\text{Si}~\text{NMR}~~(THF-}d_{8},~119~\text{MHz}):~\delta~-3.10~~(C_{5}H_{4}\text{Si}^{\prime}\text{Pr}_{3}).~\text{IR}:~3054\text{w},~2935\text{s},~2886\text{m},~2860\text{s},~1459\text{m},~1434\text{m},~1378\text{w},~1361\text{w},~1345\text{w},~1246\text{w},~1174\text{m},~1074\text{w},~1035\text{s},~1009\text{m},~979\text{w},~878\text{s},~813\text{w},~738\text{vs},~734\text{vs},~660\text{vs},~656\text{vs}.~\text{Anal.}~\text{calcd.}~\text{for}~C_{14}H_{24}\text{KSi}:~C,~64.54;~H,~9.67.~\text{Found}:~C,~65.31;~H,~9.69;~C,~65.10;~H,~9.70;~C,~65.03;~H,~9.70.~\text{The}~C/H~\text{ratios}~\text{in}~\text{the}~\text{analytical}~\text{data}~\text{give}~\text{formulas}~\text{of}~C_{14}H_{24.7},~C_{14}H_{24.7},~\text{and}~C_{14}H_{24.8},~\text{respectively},~\text{close}~\text{to}~\text{the}~\text{calculated}~\text{value}~\text{of}~C_{14}H_{25}.$

Synthesis of $(C_5H_4Si^iPr_3)_3$ ThBr, 1. $KC_5H_4Si^iPr_3$ (624 mg, 2.39 mmol) was added as a solid in portions over 1 min to a stirred white suspension of Th^{IV}Br₄(DME)₂ (584 mg, 0.798 mmol) at room temperature in Et₂O (9 mL). The resulting mixture was allowed to stir at room temperature for 16 h at which point it became a white suspension. White insoluble solids, presumably KBr, were removed by centrifugation followed by filtration to yield a clear pale-yellow solution. Solvent was removed under reduced pressure to yield white solids. The solids were extracted into hexane (5 mL) and filtered to remove insoluble solids. Solvent was removed from the clear pale-yellow filtrate to yield 1 as white solids (664 mg, 85%). Colorless crystals suitable for X-ray diffraction were grown from dilute solutions of toluene (approximately 15 mg/4 mL) stored at -35 °C. The appropriately dilute solution was obtained by repeatedly harvesting powders that initially formed from more concentrated solutions. ¹H NMR (C₆D₆, 600 MHz): δ 6.64–6.63 (m, 6H, $C_5H_4Si^3Pr_3$), 6.60–6.59 (m, 6H, $C_5H_4Si^4Pr_3$), 1.53–1.45 (sept, $^3J_{HH} = 1.2$ Hz, 9H, CH of 4Pr), 1.21–1.20 (d, ${}^{3}\vec{J}_{HH} = 1.2$ Hz, 54H, \vec{CH}_{3} of \vec{Pr}). ${}^{13}C$ NMR ($C_{6}D_{6}$, 151 MHz): δ 128.9 ($C_5H_4Si^iPr_3$), 128.6 ($C_5H_4Si^iPr_3$), 122.4 ($C_5H_4Si^iPr_3$), 19.8 (CH_3 of iPr), 12.6 (CH of iPr). ^{29}Si NMR (C_6D_6 , 119 MHz): δ – 0.86 $(C_5H_4Si^{\dagger}Pr_3)$. IR: 2941s, 2887m, 2862s, 1460m, 1382w, 1367w, 1305w, 1293w, 1242w, 1163m, 1067w, 1043s, 996m, 917w, 880s, 845w, 782vs, 778vs, 667vs, 659vs. Anal. calcd. for C₄₂H₇₅Si₃BrTh: C, 51.67; H, 7.74. Found: C, 54.42; H, 8.20; C, 52.35; H, 7.96; C, 52.78; H, 7.97. The C/ H ratios in the analytical data give formulas of C₄₂H_{75,2}, C₄₂H_{75,9}, and $C_{42}H_{75.4}$, respectively, close to the calculated value of $C_{42}H_{75}$.

Synthesis of $(C_5H_4Si^7Pr_3)_3$ Th, 2. Solid KC_8 (18 mg, 0.133 mmol) was added to a solution of $(C_5H_4Si^{\dagger}Pr_3)_3ThBr$ (104 mg, 0.106 mmol) in THF (3 mL) at room temperature to immediately produce a dark blue solution. The vial was swirled at room temperature for 5 min before being filtered to remove insoluble solids. Solvent was removed from the filtrate under reduced pressure to yield dark blue oily solids, which were then extracted into hexane (5 mL) and filtered. Solvent was removed under reduced pressure to yield dark blue solids which were then triturated with SiMe₄ (1 mL) and dried to yield (C₅H₄SiⁱPr₃)₃Th, 2, as blue solids (94 mg, 98%). Dark blue crystals suitable for X-ray diffraction were grown from a solution in pentane stored at -35 °C. ²⁹Si NMR (C_6D_{61} 119 MHz): δ –21.8 ($C_5H_4Si^iPr_3$). IR: 2941m, 2889w, 2862s, 1462m, 1382w, 1365w, 1261w, 1247w, 1159w, 1094w, 1066w, 1041s, 1015m, 997m, 917w, 880s, 860m, 841m, 769vs, 661vs, 652vs. UV—vis (THF, room temperature) $\lambda_{\rm max}$, nm (ε , M $^{-1}$ cm $^{-1}$): 350 (840, shoulder), 504 (1300), 582 (900), 664 (1100). EPR: $g_{iso} = 1.90$, $g_{||} =$ 1.97, g_{\perp} = 1.88 (100.9 mHz). Anal. calcd. for $C_{42}H_{75}Si_3Th$: C, 56.28; H, 8.43. Found: C, 56.16; H, 8.52; C, 56.36; H, 8.48; C, 55.06; H, 8.18. The C/H ratios in the analytical data give formulas of C₄₂H_{75.8}, $C_{42}H_{75.1}$, and $C_{42}H_{74.2}$, respectively, close to the calculated value of

Synthesis of [K(2.2.2-cryptand)][($C_5H_4Si^iPr_3$)₃Th], 3. Solid KC₈ (4.3 mg, 0.032 mmol) was added to a solution of 2 (24.0 mg, 0.0268 mmol) and crypt (11.0 mg, 0.0292 mmol) in THF (4 mL) at room temperature to immediately produce an inky blue-green solution. The mixture was swirled for 5 min at room temperature before being filtered to remove insoluble solids. Solvent was removed under reduced pressure to yield dark blue-black solids. The solids were then washed with hexane (2 mL) to remove unreacted 2 and dried under reduced pressure to yield 3 as dark blue-black solids (34 mg). X-ray quality crystals can be grown from a THF/hexane or diethyl ether solution stored at -35 °C. Colorless X-ray quality crystals of [K(crypt)]-[Cp^{TIPS}], identified by X-ray crystallography, were found to cocrystallize from solutions of 3 in Et₂O or THF/hexane. ¹H NMR (THF- d_8 , 600 MHz): δ 6.85–6.1 (br, 12H, $C_5H_4Si^i$ Pr₃), 3.55 (s, 12H,

 OCH_2CH_2O), 3.51 (s, 12H, NCH_2CH_2O), 2.53 (s, 12H, NCH₂CH₂O), 1.50-1.31 (br, 9H, CH of Pr), 1.30-0.98 (br, 54H, CH₃ of 'Pr). ¹³C NMR (THF- d_8 , 151 MHz): δ 114.7 ($C_5H_4Si^4Pr_3$), 107.7 ($C_5H_4Si^{\dagger}Pr_3$), 102.3 ($C_5H_4Si^{\dagger}Pr_3$), 71.3 (OCH₂CH₂O), 68.5 (NCH₂CH₂O), 54.8 (NCH₂CH₂O), 20.3 (CH₃ of ⁱPr), 13.4 (CH of ⁱPr). ²⁹Si NMR (THF- d_8 , 119 MHz): δ –5.54 (C₅H₄SiⁱPr₃). IR: 3037w, 2912w, 2883m, 2853s, 2817m, 1477w, 1460m, 1443m, 1418w, 1355s, 1296m, 1260m, 1239w, 1130s, 1101vs, 1077vs, 1033vs, 1011m, 986w, 948s, 932s, 881m, 830w, 781w, 750w, 700w, 661s. UV-vis (THF, room temperature) λ_{max} , nm (ε , M⁻¹ cm⁻¹): 424 (3910), 585 (4700, shoulder), 650 (5200). Anal. calcd. for C₆₀H₁₁₁N₂O₆Si₃KTh: C, 54.93; H: 8.53; N: 2.14. Found: C, 55.79; H, 9.95; N: 5.81. C, 55.64; H, 8.80; N, 5.971. C, 55.82, H, 8.62, N, 5.76. The C/H/N ratios in the analytical data give formulas of $C_{60}H_{127}N_{5.4}$, $C_{60}H_{113}N_{5.5}$, and $C_{60}H_{111}N_{5.3}$. The high N values can be accounted for by the presence of excess crypt (anal. calcd. for C₁₈H₃₆N₂O₆: C, 57.42; H, 9.64; N, 7.44) in crystalline samples of 3.

Independent Synthesis of Crystallographically Characterized [K(2.2.2-cryptand)][$C_5H_4Si^iPr_3$]. $KC_5H_4Si^iPr_3$ (16.0 mg, 0.0614 mmol) and 2.2.2-cryptand (23.0 mg, 0.0614 mmol) were both added to a J. Young NMR tube fitted with a Teflon stopper. THF- d_8 (1 mL) and one drop of SiMe₄ were then added to the J. Young tube, and the tube was shaken until all the solids were dissolved to form a colorless solution. NMR spectroscopy confirmed the quantitative formation of [K(2.2.2-cryptand)][$C_5H_4Si^iPr_3$]. ¹H NMR (THF- d_8 , 600 MHz): δ 5.81 (m, 2H, $C_5H_4Si^iPr_3$), 5.66 (m, 2H, $C_5H_4Si^iPr_3$), 3.46 (s, 12H, NCH_2CH_2O), 3.44 (t, ${}^3J_{HH}$ = 3.4 Hz, 12H, NCH_2CH_2O), 2.47 (t, ${}^3J_{HH}$ = 2.4 Hz, 12H, NC H_2 CH $_2$ O), 1.17–1.11 (sept, $^3J_{HH}$ = 1.1 Hz, 3H, CH of Pr), 1.07 (d, $^3J_{HH}$ = 1.1 Hz, 18H, C H_3 of Pr). 13 C NMR (THF- d_8) 151 MHz): δ 113.8 ($C_5H_4Si^iPr_3$), 106.7 ($C_5H_4Si^iPr_3$), 99.0 $(C_5H_4Si^{i}Pr_3)$, 71.3 (OCH₂CH₂O), 68.4 (NCH₂CH₂O), 54.9 (NCH₂CH₂O), 20.5 (CH₃ of ⁱPr), 13.7 (CH of ⁱPr). ²⁹Si NMR (THF- d_8 , 119 MHz): δ –3.52 (C₅H₄Si[†]Pr₃). Crystal data, bond length and angle tables, and structure refinement information can be found in the Supporting Information.

ASSOCIATED CONTENT

Supporting Information

The Supporting Information is available free of charge at https://pubs.acs.org/doi/10.1021/acs.organomet.3c00343.

 $G\,e\,o\,m\,e\,t\,r\,y\,-\,o\,p\,t\,i\,m\,i\,z\,e\,d$ coordinates for $[(C_5H_4Si^IPr_3)_3Th^{II}]^{1-}\,(XYZ)$

Geometry-optimized coordinates for $(C_5H_4Si^iPr_3)_3Th^{III}$ (XYZ)

Spectra (NMR, infrared, and EPR), cyclic voltammograms, crystallographic data, thermal decomposition pictures, and computational details (PDF)

Accession Codes

CCDC 2266478, 2266479, 2266481, 2266542, 2267246, and 2268379 contain the supplementary crystallographic data for this paper. These data can be obtained free of charge via www.ccdc.cam.ac.uk/data_request/cif, or by emailing data_request@ccdc.cam.ac.uk, or by contacting The Cambridge Crystallographic Data Centre, 12 Union Road, Cambridge CB2 1EZ, U.K.; Fax: +44-1223-336033. Crystal data, bond lengths and angles tables, and structure refinement information can be found in the Supporting Information.

AUTHOR INFORMATION

Corresponding Authors

William J. Evans — Department of Chemistry, University of California, California 92697-2025, United States;
orcid.org/0000-0002-0651-418X; Email: wevans@uci.edu

Filipp Furche — Department of Chemistry, University of California, California 92697-2025, United States;
orcid.org/0000-0001-8520-3971; Email: filipp.furche@

Authors

Joseph Q. Nguyen — Department of Chemistry, University of California, California 92697-2025, United States;
orcid.org/0000-0001-8058-7099

Lauren M. Anderson-Sanchez – Department of Chemistry, University of California, California 92697-2025, United States; orcid.org/0000-0002-9697-8008

William N. G. Moore — Department of Chemistry, University of California, California 92697-2025, United States;
orcid.org/0000-0001-5074-9341

Joseph W. Ziller – Department of Chemistry, University of California, California 92697-2025, United States;
occid.org/0000-0001-7404-950X

Complete contact information is available at: https://pubs.acs.org/10.1021/acs.organomet.3c00343

Notes

The authors declare the following competing financial interest(s): Principal Investigator Filipp Furche has an equity interest in TURBOMOLE GmbH. The terms of this arrangement have been reviewed and approved by the University of California, Irvine, in accordance with its conflict of interest policies.

ACKNOWLEDGMENTS

The authors thank the Chemical Sciences, Geosciences, and Biosciences Division of the Office of Basic Energy Sciences of the U.S. Department of Energy for support of the experimental parts of this study through DE-SC0004739 (to W.J.E.). The theoretical studies reported here were supported by the National Science Foundation under CHE-2102568 (to F.F.). They also thank Prof. Andrew S. Borovik for spectroscopic (EPR) assistance.

REFERENCES

- (1) Manriquez, J. M.; Fagan, P. J.; Marks, T. J.; Vollmer, S. H.; Secaur Day, C.; Day, V. W. Pentamethylcyclopentadienyl organoactinides. Trivalent uranium organometallic chemistry and the unusual structure of bis(pentamethylcyclopentadienyl)uranium monochloride. *J. Am. Chem. Soc.* **1979**, *101*, 5075–5078.
- (2) Männig, D.; Nöth, H. Metallboranate und Boranatometallate. 13 [1]. Darstellung und Molekülstruktur von Uran(III)-tetrahydridoborat-3-Tetrahydrofuran. *Z. Anorg. Allg. Chem.* **1986**, 543, 66–72.
- (3) Zalkin, A.; Brennan, J. G.; Andersen, R. A. Tris-(trimethylsilylcyclopentadienyl)uranium(III). *Acta Crystallogr. C* 1988, 44, 2104–2106.
- (4) Clark, D. L.; Sattelberger, A. P.; Van der Sluys, W. G.; Watkin, J. G. New developments in actinide alkoxide chemistry. *J. Alloys Compd.* **1992**, *180*, 303–315.
- (5) Roussel, P.; Scott, P. Complex of Dinitrogen with Trivalent Uranium. J. Am. Chem. Soc. 1998, 120, 1070-1071.
- (6) Daly, S. R.; Girolami, G. S. Synthesis, Characterization, and Structures of Uranium(III) *N,N*-Dimethylaminodiboranates. *Inorg. Chem.* **2010**, 49, 5157–5166.
- (7) Evans, W. J.; Kozimor, S. A. Expanding the chemistry of U³⁺ Reducing agents. *Coord. Chem. Rev.* **2006**, *250*, 911–935.
- (8) Baker, R. J. The coordination and organometallic chemistry of UI₃ and U{N(SiMe₃)₂}₃: Synthetic Reagents par excellence. *Coord. Chem. Rev.* **2012**, 256, 2843–2871.

- (9) Boreen, M. A.; Arnold, J. The synthesis and versatile reducing power of low-valent uranium complexes. *Dalton Trans.* **2020**, 49, 15124–15138.
- (10) Blake, P. C.; Lappert, M. F.; Atwood, J. L.; Zhang, H. The Synthesis and Characterisation, Including X-Ray Diffraction Study, of $[Th\{\eta^5-C_5H_3(SiMe_3)_2\}_3]$; the First Thorium(III) Crystal Structure. *J. Chem. Soc. Chem. Commun.* **1986**, *15*, 1148–1149.
- (11) Huh, D. N.; Roy, S.; Ziller, J. W.; Furche, F.; Evans, W. J. Isolation of a Square-Planar Th(III) Complex: Synthesis and Structure of [Th(OC₆H₂^tBu₂-2,6-Me-4)₄]¹⁻. *J. Am. Chem. Soc.* **2019**, *141*, 12458–12463
- (12) Blake, P. C.; Edelstein, N. M.; Hitchcock, P. B.; Kot, W. K.; Lappert, M. F.; Shalimoff, G. V.; Tian, S. Synthesis, Properties and Structures of the Tris(Cyclopentadienyl) Thorium(III) Complexes $[Th\{\eta^5-C_5H_3(SiMe_2R)_2-1,3\}_3]$ (R = Me or ^tBu). *J. Organomet. Chem.* **2001**, 636, 124–129.
- (13) Langeslay, R. R.; Fieser, M. E.; Ziller, J. W.; Furche, F.; Evans, W. J. Expanding Thorium Hydride Chemistry Through Th²⁺, Including the Synthesis of a Mixed-Valent Th⁴⁺/Th³⁺ Hydride Complex. *J. Am. Chem. Soc.* **2016**, *138*, 4036–4045.
- (14) Langeslay, R. R.; Chen, G. P.; Windorff, C. J.; Chan, A. K.; Ziller, J. W.; Furche, F.; Evans, W. J. Synthesis, Structure, and Reactivity of the Sterically Crowded Th^{3+} Complex $(C_5\operatorname{Me}_5)_3\operatorname{Th}$ Including Formation of the Thorium Carbonyl, $[(C_5\operatorname{Me}_5)_3\operatorname{Th}(CO)][BPh_4]$. *J. Am. Chem. Soc.* **2017**, *139*, 3387–3398.
- (15) Parry, J. S.; Cloke, F. G. N.; Coles, S. J.; Hursthouse, M. B. Synthesis and Characterization of the First Sandwich Complex of: Trivalent Thorium: A Structural Comparison with the Uranium Analogue. J. Am. Chem. Soc. 1999, 121, 6867–6871.
- (16) Walensky, J. R.; Martin, R. L.; Ziller, J. W.; Evans, W. J. Importance of Energy Level Matching for Bonding in Th^{3+} -Am $^{3+}$ Actinide Metallocene Amidinates, $(C_5Me_5)_2[$ i PrNC(Me)N i Pr]An. *Inorg. Chem.* **2010**, 49, 10007–10012.
- (17) Siladke, N. A.; Webster, C. L.; Walensky, J. R.; Takase, M. K.; Ziller, J. W.; Grant, D. J.; Gagliardi, L.; Evans, W. J. Actinide Metallocene Hydride Chemistry: C-H Activation in Tetramethylcyclopentadienyl Ligands to Form $[\mu\text{-H}_5\text{-C}_5\text{Me}_3\text{H}(\text{CH}_2)\text{-}\kappa\text{C}]^{2-}$ Tuckover Ligands in a Tetrathorium Octahydride Complex. *Organometallics* **2013**, *32*, 6522–6531.
- (18) Altman, A. B.; Brown, A. C.; Rao, G.; Lohrey, T. D.; Britt, R. D.; Maron, L.; Minasian, S. G.; Shuh, D. K.; Arnold, J. Chemical Structure and Bonding in a Thorium(III)-Aluminum Heterobimetallic Complex. *Chem. Sci.* **2018**, *9*, 4317–4324.
- (19) Formanuik, A.; Ariciu, A. M.; Ortu, F.; Beekmeyer, R.; Kerridge, A.; Tuna, F.; McInnes, E. J. L.; Mills, D. P. Actinide Covalency Measured by Pulsed Electron Paramagnetic Resonance Spectroscopy. *Nat. Chem.* **2017**, *9*, 578–583.
- (20) Boronski, J. T.; Seed, J. A.; Hunger, D.; Woodward, A. W.; van Slageren, J.; Wooles, A. J.; Natrajan, L. S.; Kaltsoyannis, N.; Liddle, S. T. A crystalline tri-thorium cluster with σ -aromatic metal—metal bonding. *Nature* **2021**, *598*, 72–75.
- (21) Wedal, J. C.; Bekoe, S.; Ziller, J. W.; Furche, F.; Evans, W. J. In search of tris(trimethylsilylcyclopentadienyl)thorium. *Dalton. Trans.* **2019**, *48*, 16633–16640.
- (22) La Pierre, H. S.; Scheurer, A.; Heinemann, F. W.; Hieringer, W.; Meyer, K. Synthesis and Characterization of a Uranium(II) Monoarene Complex Supported by δ Backbonding. *Angew. Chem., Int. Ed.* **2014**, 53, 7158–7162.
- (23) Billow, B. S.; Livesay, B. N.; Mokhtarzadeh, C. C.; McCracken, J.; Shores, M. P.; Boncella, J. M.; Odom, A. L. Synthesis and Characterization of a Neutral U(II) Arene Sandwich Complex. *J. Am. Chem. Soc.* **2018**, *140*, 17369–17373.
- (24) Straub, M. D.; Ouellette, E. T.; Boreen, M. A.; Britt, R. D.; Chakarawet, K.; Iskander, D.; Gould, C. A.; Maron, L.; Del Rosal, I.; Villarreal, D.; Minasian, S. G.; Arnold, J. A Uranium(II) Arene Complex That Acts as a Uranium(I) Synthon. *J. Am. Chem. Soc.* **2021**, *143*, 19748–19760.

- (25) Guo, F.-S.; Tsoureas, N.; Huang, G.-Z.; Tong, M.-L.; Mansikkamäki, A.; Layfield, R. A. Isolation of a Perfectly Linear Uranium(II) Metallocene. *Angew. Chem., Int. Ed.* **2020**, 59, 2299–2303.
- (26) Ryan, A. J.; Angadol, M. A.; Ziller, J. W.; Evans, W. J. Isolation of U(II) Compounds Using Strong Donor Ligands, C_5Me_4H and N(SiMe₃)₂, Including a Three-Coordinate U(II) Complex. *Chem. Commun.* **2019**, 55, 2325–2327.
- (27) Modder, D. K.; Palumbo, C. T.; Douair, I.; Fadaei-Tirani, F.; Maron, L.; Mazzanti, M. Delivery of a Masked Uranium(II) by an Oxide-Bridged Diuranium (III) Complex. *Angew. Chem., Int. Ed.* **2021**, 60, 3737–3744.
- (28) MacDonald, M. R.; Fieser, M. E.; Bates, J. E.; Ziller, J. W.; Furche, F.; Evans, W. J. Identification of the +2 Oxidation State for Uranium in a Crystalline Molecular Complex, [K(2.2.2-cryptand)]- $[(C_5H_4\text{SiMe}_3)_3\text{U}]$. J. Am. Chem. Soc. 2013, 135, 13310–13313.
- (29) Langeslay, R. R.; Fieser, M. E.; Ziller, J. W.; Furche, F.; Evans, W. J. Synthesis, Structure, and Reactivity of Crystalline Molecular Complexes of the $\{[C_5H_3(SiMe_3)_2]_3Th\}^{1-}$ Anion Containing Thorium in the Formal + 2 Oxidation State. *Chem. Sci.* **2015**, *6*, 517–521.
- (30) Wedal, J. C.; Barlow, J. M.; Ziller, J. W.; Yang, J. Y. Electrochemical studies of tris(cyclopentadienyl) thorium and uranium complexes in the + 2, + 3, and + 4 oxidation states. *Chem. Sci.* **2021**, *12*, 8501–8511.
- (31) Cassani, M. C.; Duncalf, D. J.; Lappert, M. F. The First Example of a Crystalline Subvalent Organolanthanum Complex: $[K([18]\text{crown-}6)-(\eta^2-C_6H_6)_2][(LaCp^{tt}_2)_2(\mu-\eta^6:\eta^6-C_6H_6)]\bullet 2C_6H_6$ ($Cp^{tt}=\eta^5-C_5H_3Bu^t_2-1,3$). *J. Am. Chem. Soc.* **1998**, *120*, 12958–12959.
- (32) Moehring, S. A.; Miehlich, M.; Hoerger, C. J.; Meyer, K.; Ziller, J. W.; Evans, W. J. A Room-Temperature Stable Y(II) Aryloxide: Using Steric Saturation to Kinetically Stabilize Y(II) Complexes. *Inorg. Chem.* **2020**, *59*, 3207–3214.
- (33) Anderson-Sanchez, L. A.; Yu, J. M.; Ziller, J. W.; Furche, F.; Evans, W. J. Room-Temperature Stable Ln(II) Complexes Supported by 2,6-Diadamantyl Aryloxide Ligands. *Inorg. Chem.* **2023**, *62*, 706–714.
- (34) Guzei, I. A.; Wendt, M. An improved method for the computation of ligand steric effects based on solid angles. *Dalton Trans.* **2006**, 33, 3991–3999.
- (35) Kahan, R. J.; Farnaby, J. H.; Tsoureas, N.; Cloke, F. G. N.; Hitchcock, P. B.; Coles, M. P.; Roe, S. M.; Wilson, C. Sterically encumbered mixed sandwich compounds of uranium(II): Synthesis and reactivity with small molecules. *J. Organomet. Chem.* **2018**, 857, 110–122.
- (36) Schüler, P.; Görls, H.; Krieck, S.; Westerhausen, M. One-Step Synthesis and Schlenk-Type Equilibrium of Cyclopentadienylmagnesium Bromides. *Chem.—Eur. J.* **2021**, *27*, 15508–15515.
- (37) Edelman, M. A.; Hitchcock, P. B.; Lappert, M. F.; Liu, D.-S.; Tian, S. Synthesis and characterization of trimethylsilylmethylbis(trimethylsilyl)methyland silyl-substituted cyclopentadienes and their alkali metal complexes. *J. Organomet. Chem.* **1998**, 550, 397–408.
- (38) Ren, W.; Zhao, N.; Chen, Liang; Song, H.; Zi, G. Synthesis, structure, and catalytic activity of an organothorium hydride complex. *Inorg. Chem. Commun.* **2011**, *14*, 1838–1841.
- (39) Blake, P. C.; Edelman, M. A.; Hitchcock, P. B.; Hu, J.; Lappert, M. F.; Tian, S.; Müller, G.; Atwood, J. L.; Zhang, H. Organometallic chemistry of the actinides: Part 4 The chemistry of some tris-(cyclopentadienyl)actinide complexes. *J. Organomet. Chem.* 1998, 551, 261–270.
- (40) Windorff, C. J.; MacDonald, M. R.; Ziller, J. W.; Evans, W. J. Trimethylsilyl (Cp') Uranium Chemistry: Synthetic and Structural Studies of Cp'_4U and Cp'_3UX (X = Cl, I, Me). Z. Anorg. Allg. Chem. **2017**, 643, 2011–2018.
- (41) Lok, M. T.; Tehan, F. J.; Dye, J. L. Spectra of Na-, K-, and e-solv in amines and ethers. J. Phys. Chem. 1972, 76, 2975–2981.
- (42) Nakamoto, K. Infrared Spectra of Inorganic and Coordination Compounds, 2nd ed; John Wiley and Sons, 1970; pp. 214.
- (43) Fieser, M. E.; MacDonald, M. R.; Krull, B. T.; Bates, J. E.; Ziller, J. W.; Furche, F.; Evans, W. J. Structural, Spectroscopic, and Theoretical Comparison of Traditional vs Recently Discovered Ln²⁺ Ions in the

- [K(2.2.2-cryptand]]($(C_5H_4SiMe_3)_3Ln$] Complexes: The Variable Nature of Dy^{2+} and Nd^{2+} . *J. Am. Chem. Soc.* **2015**, 137, 369–382.
- (44) Evans, W. J. Tutorial on the Role of Cyclopentadienyl Ligands in the Discovery of Molecular Complexes of the Rare-Earth and Actinide Metals in New Oxidation States. *Organometallics* **2016**, *35*, 3088–3100.
- (45) Macdonald, M. R.; Fieser, M. E.; Bates, J. E.; Ziller, J. W.; Furche, F.; Evans, W. J. Identification of the +2 Oxidation State for Uranium in a Crystalline Molecular Complex, [K(2.2.2-cryptand)]- $[(C_5H_4\text{SiMe}_3)_3\text{U}]$. J. Am. Chem. Soc. 2013, 135, 13310–13313.
- (46) Windorff, C. J.; MacDonald, M. R.; Meihaus, K. R.; Ziller, J. W.; Long, J. R.; Evans, W. J. Expanding the Chemistry of Molecular U^{2+} Complexes: Synthesis, Characterization, and Reactivity of the $\{[C_5H_3(SiMe_3)_2]_3U\}^{1-}$ Anion. *Chem.—Eur. J.* **2015**, 22, 772–782.
- (47) Staroverov, V. N.; Scuseria, G. E.; Tao, J.; Perdew, J. P. Comparative Assessment of a New Nonempirical Density Functional: Molecules and Hydrogen-Bonded Complexes. *J. Chem. Phys.* **2003**, *119*, 12129–12137.
- (48) Grimme, S.; Antony, J.; Ehrlich, S.; Krieg, H. A Consistent and Accurate Ab Initio Parametrization of Density Functional Dispersion Correction (DFT-D) for the 94 Elements H-Pu. *J. Chem. Phys.* **2010**, 132, 154104.
- (49) Grimme, S. Semiempirical GGA-Type Density Functional Constructed with a Long-Range Dispersion Correction. *J. Comput. Chem.* **2006**, *27*, 1787–1799.
- (50) Weigend, F.; Köhn, A.; Hättig, C. Efficient Use of the Correlation Consistent Basis Sets in Resolution of the Identity MP2 Calculations. *J. Chem. Phys.* **2002**, *116*, 3175–3183.
- (51) Cao, X.; Dolg, M. Segmented Contraction Scheme for Small-Core Actinide Pseudopotential Basis Sets. *J. Mol. Struct. Theochem.* **2004**, *673*, 203–209.
- (52) Eichkorn, K.; Weigend, F.; Treutler, O.; Ahlrichs, R. Auxiliary Basis Sets for Main Row Atoms and Transition Metals and Their Use to Approximate Coulomb Potentials. *Theor. Chem. Acc.* **1997**, 97, 119–124.
- (53) Schäfer, A.; Klamt, A.; Sattel, D.; Lohrenz, J. C. W.; Eckert, F. COSMO Implementation in TURBOMOLE: Extension of an Efficient Quantum Chemical Code towards Liquid Systems. *Phys. Chem. Chem. Phys.* **2000**, *2*, 2187–2193.
- (54) CRC Handbook of Chemistry and Physics, 97th ed.; Haynes, W. M., Lide, D. R., Bruno, T. J., Eds.; CRC Press, 2016.
- (55) TURBOMOLE V7.6 2020, a development of University of Karlsruhe and Forschungszentrum Karlsruhe GmbH, 1989–2007, TURBOMOLE GmbH, since 2007: available from http://www.turbomole.com (accessed January 2023 to April 2023).
- (56) Balasubramani, S. G.; Chen, G. P.; Coriani, S.; Diedenhofen, M.; Frank, M. S.; Franzke, Y. J.; Furche, F.; Grotjahn, R.; Harding, M. E.; Hättig, C.; Hellweg, A.; Helmich-Paris, B.; Holzer, C.; Huniar, U.; Kaupp, M.; Marefat Khah, A.; Karbalaei Khani, S.; Müller, T.; Mack, F.; Nguyen, B. D.; Parker, S. M.; Perlt, E.; Rappoport, D.; Reiter, K.; Roy, S.; Rückert, M.; Schmitz, G.; Sierka, M.; Tapavicza, E.; Tew, D. P.; Van Wüllen, C.; Voora, V. K.; Weigend, F.; Wodyński, A.; Yu, J. M. TURBOMOLE: Modular Program Suite for Ab Initio Quantum-Chemical and Condensed-Matter Simulations. *J. Chem. Phys.* 2020, 152, 184107.
- (57) Evans, W. J.; Davis, B. L. Chemistry of Tris-(pentamethylcyclopentadienyl) f-Element Complexes, (C₅Me₅)₃M. *Chem. Rev.* **2002**, *102*, 2119–2136.
- (58) (a) Nguyen, J. Q.; Evans, W. J. unpublished results.. (b) Langeslay, R. R. Expanding the Fundamental Chemistry of Thorium Through the Synthesis and Reactivity of the First Molecular Complexes of Th(II) and New Classes of Th(III) and Th(IV) Compounds; University of California, 2016
- (59) Rücker, C. The Triisopropylsilyl Group in Organic Chemistry: Just a Protective Group, or More? *Chem. Rev.* **1995**, *95*, 1009–1064.
- (60) Panda, T. K.; Gamer, M. T.; Roesky, P. W. An Improved Synthesis of Sodium and Potassium Cyclopentadienide. *Organometallics* **2003**, 22, 877–878.
- (61) Bergbreiter, D. E.; Killough, J. M. Reactions of potassium-graphite. J. Am. Chem. Soc. 1978, 100, 2126–2134.

(62) Clark, D. L.; Frankcom, T. M.; Miller, M. M.; Watkin, J. G. Facile solution routes to hydrocarbon-soluble Lewis base adducts of thorium tetrahalides. Synthesis, characterization, and x-ray structure of ThBr₄(THF)₄. *Inorg. Chem.* **1992**, *31*, 1628–1633.